Bull Earthquake Eng (2017) 15:313–337
DOI 10.1007/s10518-016-9970-z

ORIGINAL RESEARCH PAPER

Dynamic investigation on the Mirandola bell tower in post-earthquake scenarios

Luca Zanotti Fragonara[1] · Giosuè Boscato[2] · Rosario Ceravolo[3] · Salvatore Russo[2] · Silvia Ientile[4] · Marica Leonarda Pecorelli[3] · Antonino Quattrone[3]

Received: 22 December 2015 / Accepted: 10 July 2016 / Published online: 19 July 2016
© The Author(s) 2016. This article is published with open access at Springerlink.com

Abstract After the seismic events of the 20th and 29th of May 2012 in Emilia (Italy), most of the monumental and historic buildings of the area were severely damaged. In a few structures, partial collapse mechanisms were observed (e.g. façade tilting, out-of-plane overturning of panels…). This paper presents the case-study of the bell tower of the Santa Maria Maggiore cathedral, located in Mirandola (Italy). The dynamic response of the structure was evaluated through operational modal analysis using ambient vibrations, a consolidated non-destructive procedure that estimates the dynamic parameters of the bell-tower. The dynamic tests were carried out in pre-intervention and post-intervention conditions in order to understand the sensitivity of dynamic measurements to safety interventions. Furthermore, a comparative study is made with similar cases of undamaged masonry towers up to the 6th mode. Finally, an investigation on the state of connections and of the building itself is carried out via FE model updating.

Keywords Structures · Cultural heritage · Structural identification · Model updating · Post-earthquake safety intervention · Vibration methods · 2012 Emilia earthquake

✉ Luca Zanotti Fragonara
l.zanottifragonara@cranfield.ac.uk; lucazanottifragonara@gmail.com

[1] School of Aerospace, Transportation and Manufacturing, Cranfield University, Cranfield, UK

[2] Laboratory of Strength of Materials, IUAV University of Venice, Via Torino 153/A, 30173 Mestre, Venice, Italy

[3] Department of Structural, Building and Geotechnical, Politecnico di Torino, Corso Duca degli Abruzzi 24, 10129 Turin, Italy

[4] Department of Design and Planning in Complex Environments, IUAV University of Venice, Dorsoduro 2206, 30123 Venice, Italy

1 Introduction

Masonry heritage structures are among the most vulnerable typologies when seismic swarms strike the territory. It is not rare that aftershocks may cause more damage than the main shock itself on this typology (e.g. due to accumulated damage in masonry or due to damage on the structure that exposes vulnerabilities). In the first phase of a post-earthquake emergency, one of the most critical problems of authorities and technicians is securing damaged structures by means of temporary interventions (e.g. demolition, shoring, installation of metal rods, and hoops, etc.). In fact, timely provisional interventions are often required in post-seismic scenarios. Their aim is to avoid further damage (or even the full collapse) to the structure due to aftershocks or to other external sources (e.g. atmospheric agents, etc.). The complexity is due to the choice of the adequate type of intervention for that particular type of structure, the performance and the cost of it. This latter point is relevant, especially considering the number of operations carried out after an earthquake that are generally going to be removed in the permanent repair phase. Moreover, the typology of intervention is often chosen by just resorting to static considerations or by mechanism that can be triggered by the seismic event. The real dynamic of the system is typically not considered due to lack of time and structural complexity. A promising way to meet both the requirements could push through the application of vibration-based monitoring (VBM) systems, inasmuch as they allow to investigate the global response of a structure, highlighting the occurrence of damages, their typologies and evolutions (Russo 2013). In fact, dynamic monitoring systems have proven to be particularly suited for cultural heritage structures such as palaces, churches and towers, whose structural behaviour is strongly influenced by their geometric complexity, the nonlinearity and inhomogeneity of masonry material (Ceravolo et al. 2016). In particular, because of their non-destructive and non-invasive nature, vibration-based monitoring can be safely applied to damaged structures, potentially dangerous under other test conditions. Furthermore, the analysis of vibration data can reveal the structural weaknesses or deficiencies induced by the seismic event. In fact, the monitoring of a set of appropriately chosen features, capable to seize the global or local structural weaknesses, may reveal the effectiveness of the safety and retrofitting interventions or the progression in structural damage (Ceravolo et al. 2016). For their non-invasive peculiarities the VBM procedures are widely used in historic masonry structures. Several researches have addressed structural identification of cultural heritage using ambient vibration data (Pau and Vestroni 2008; Casciati and Faravelli 2010; Ramos et al. 2010; Pau and Vestroni 2013).

This paper proposes a benchmark study for VBM applied to the bell-tower of Santa Maria Maggiore Cathedral in Mirandola (Italy), which was heavily damaged by the 2012 Emilia earthquake sequence. In fact, valuable data gathered during two testing campaigns on the structure evidenced a correlation of different modal features with the post-earthquake scenario. A first dynamic test campaign, conducted in the aftermath of the earthquake, allowed to identify the modal parameters related to the damaged state of the tower bell, whereas the analysis of vibration data collected during a second campaign showed how the provisional interventions influenced the dynamic behaviour, increasing the global stiffness and varying the modal shapes of the structure.

2 Case study: bell-tower of Mirandola

The construction of the bell-tower of S. Maria Maggiore cathedral in Mirandola (Modena, Italy) (Fig. 1) started in the late fourteenth century. The bell-tower, made of brick masonry, is located on the south-east side of the cathedral. It is square in plan with dimension of 5.90 m and has a current height of 48 m. The building, like the whole cathedral, is the result of several alterations which occurred over the centuries. The most relevant modifications were made in the seventeenth century when the height of the original tower was tripled (Ceretti 1889) and the structure was reinforced and partially rebuilt to withstand the new loads. Another important alteration dates back to the eighteenth century, when the bell-tower was completed with an octagonal stone roofing.

The bell tower has two orders of large openings close to the top, unusually the larger ones are at the lower level (21 m) and the top ones at the belfry level (30.5 m). In the

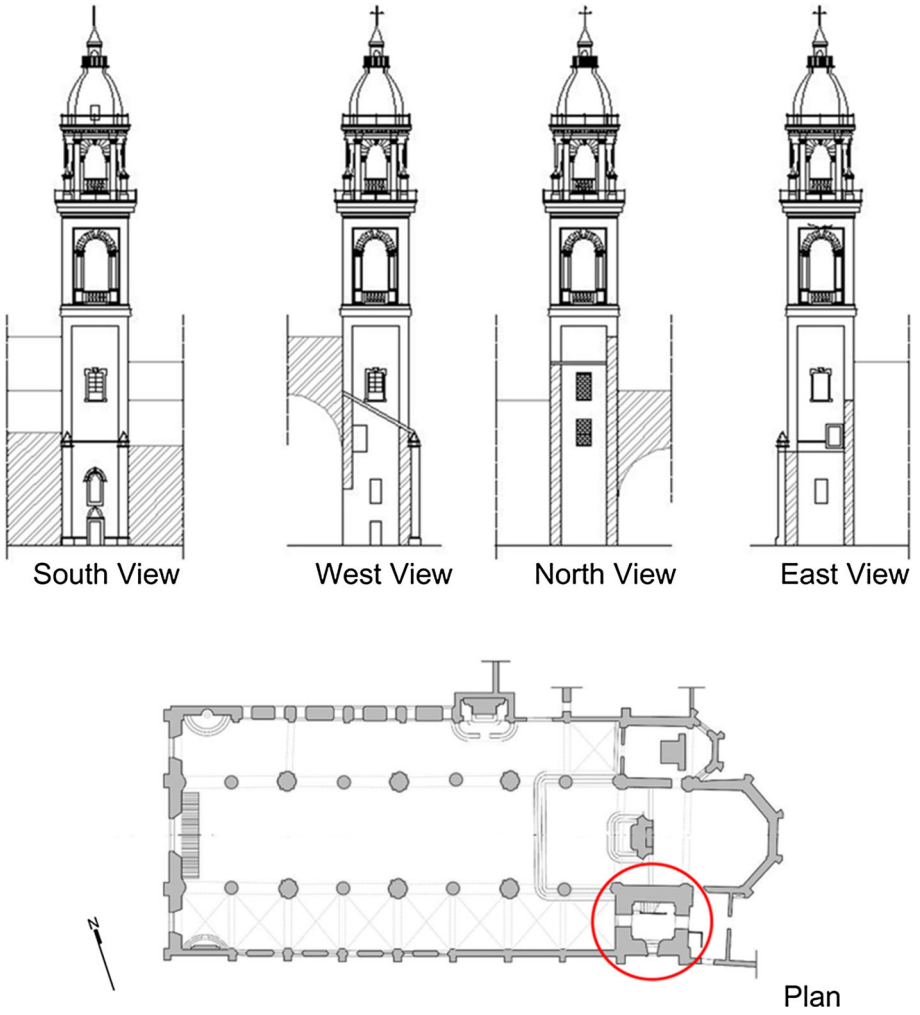


Fig. 1 Main fronts of the bell-tower and plan

bottom part of the tower there are other modestly sized openings and some of these have been successively walled up. The internal flooring of the tower bell are masonry vaults, as visually confirmed by a post-earthquake survey. Moreover, a series of small stone flights of stairs connects the various levels of the structure up to the belfry. There is no information available about the foundations of the tower to the authors. The geologic settings of the area of Mirandola were analysed by Milana et al. (2014). The area of Mirandola is characterized by a modest historical seismicity. Until the 2012 Emilia Earthquake in which the maximum intensities were recorded, the seismic events occurred did not cause significant damages to the tower.

2.1 Damage after the 2012 Emilia Earthquake

The May 2012 Emilia earthquake sequence severely damaged the cathedral, with two events on May 20th and 29th. The epicentre of the May 29th event was less than 1 km far from the site of the bell tower, which led to massive destruction to the historical city centre of Mirandola. It resulted in the collapse of the aisle, the side aisle, the roof and in several cracks on the bell-tower (Fig. 2).

An exterior laser scanner survey of the cracking patterns, carried out by the INGV (Istituto Nazionale di Geofisica e Vulcanologia) within the ILRIS 3D project (Pesci et al. 2012), highlighted the activation of a twisting mechanism leading to a rotation of about 1 degree of the building portion located between 20 and 32 m. The structural damages are mainly concentrated in this section of the bell tower, where deep diagonal cracks right below the first order of openings on all four sides can be noted, extending down to the openings of the underlying level. Furthermore, various lintels failed on the South, West and East fronts. The twisting mechanism and the high local stresses caused the crushing of masonry near the area of the tower in contact with the adjacent building, especially at the

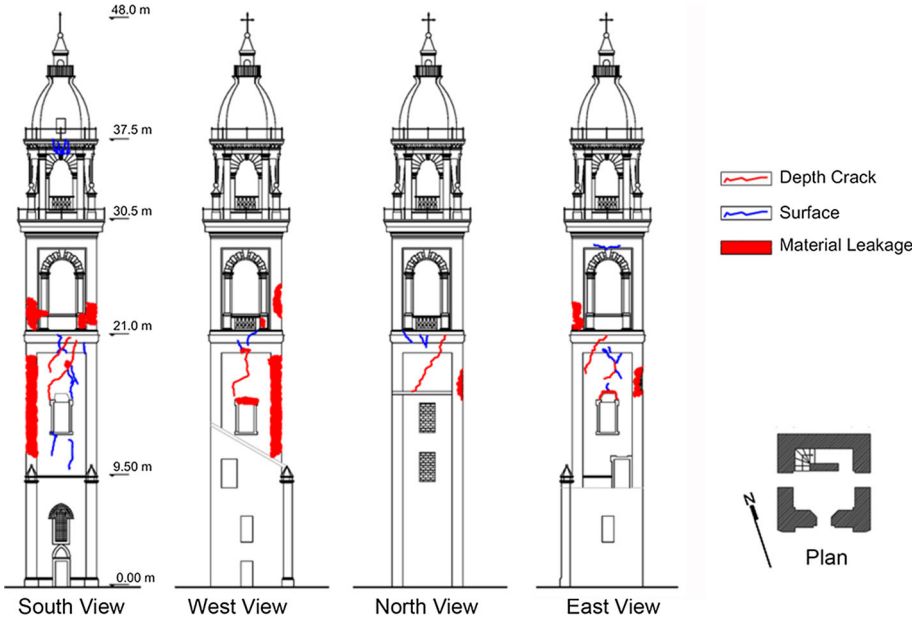


Fig. 2 Post-earthquake damage survey of the Mirandola bell-tower

height of 21 m (Fig. 3a, b). Metal chains were revealed by the occurred damages inside the masonry layer around the perimeter at the base of this level of the structure, as shown in (Fig. 3c). The visual and laser scanner surveys did not confirm for the other levels.

The internal state of the bell tower was assessed by visual inspection and this was compared to the laser scanner survey. Only two masonry vaults in the basement are still standing with clearly visible cracks (Fig. 4a, b). The internal staircases are partially collapsed and only the flight between 0 and 9.5 m (Fig. 4c) is still accessible. From this level up to the belfry all ceilings and stairs are collapsed as can be seen in Fig. 4d which depicts the remains of a flight of stairs at 9.5 m of height.

2.2 Provisional safety interventions

In order to guarantee the stability of the building and to avoid further damages, provisional post-earthquake safety interventions were put in place by the authorities between the 14th and the 18th August 2012. The bell-tower of S. Maria Maggiore was reinforced with eight metal tie-rods located at two levels of the structure (see Fig. 5-1). Moreover, the main and large openings were reinforced using wooden falseworks, as shown in Fig. 5-2, 3, together with wooden ribs in the smaller openings (Fig. 5-4).

3 Operational modal analysis

The authorities ordered safety interventions in order to prevent the collapse of the cathedral and of the bell tower immediately after the first emergency phase. A temporary vibration monitoring system was put in place before and after the installation of the safety interventions in order to investigate and validate the dynamic behaviour of the bell-tower in the two scenarios.

3.1 Dynamic monitoring

A first test campaign was carried out on the damaged structure after the main seismic events on the August 2012 by the laboratory of Strength of Materials of the IUAV (Istituto

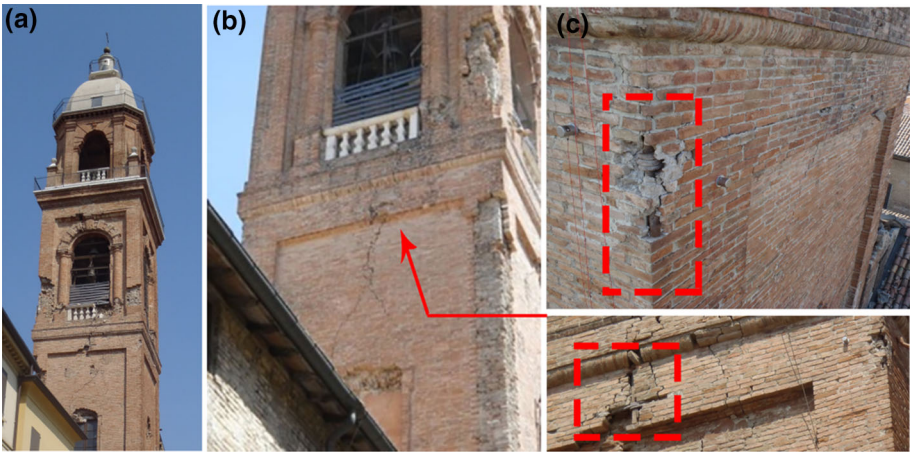


Fig. 3 Damage at the level of the belfry of the bell-tower (**a**, **b**) and the metal chains (**c**) at 20 m

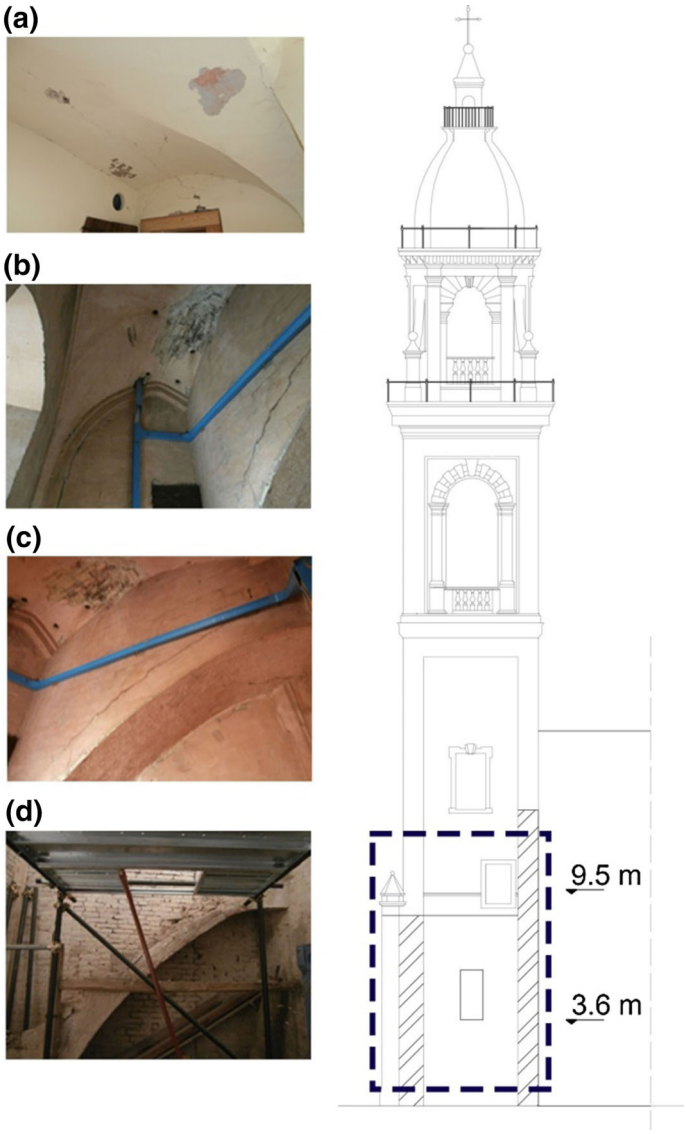


Fig. 4 Damage on vaulted slabs at 3.6 m (**a**) and at 9.5 m (**b**) and internal staircase (**c**, **d**)

Universitario di Venezia—University). A second test was carried out in September 2012, after the post-earthquake safety interventions. The dynamic responses to ambient noise were recorded. The experimental setup was designed to investigate the global dynamic behaviour of the tower, as far as was possible by the precarious structural conditions. The accelerometers were placed at different levels of the south side and at two levels on the east side. The test setup, as presented in Fig. 6, was constituted by eight uniaxial piezoelectric accelerometers (PCB Piezotronics type 393C) with a nominal sensitivity of about 1 V/g, and a measurement range of ± 2.5 g peak.

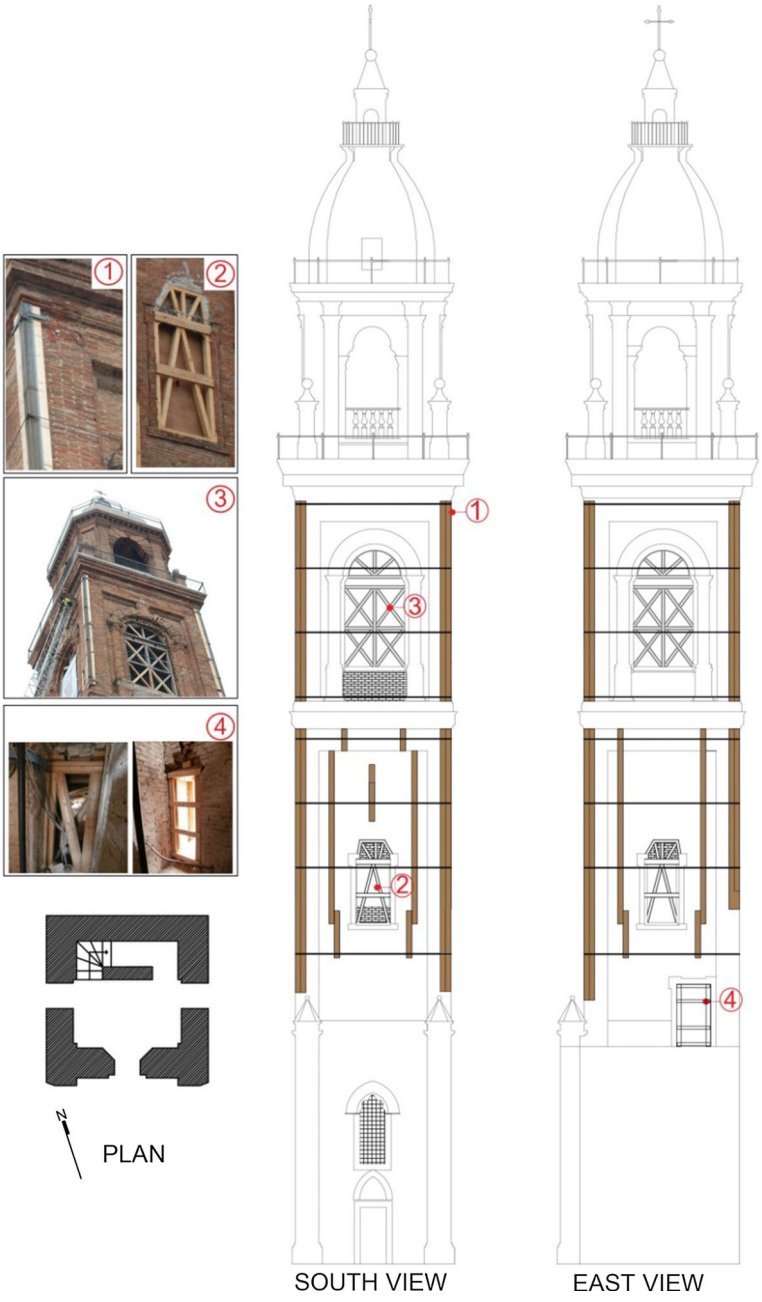
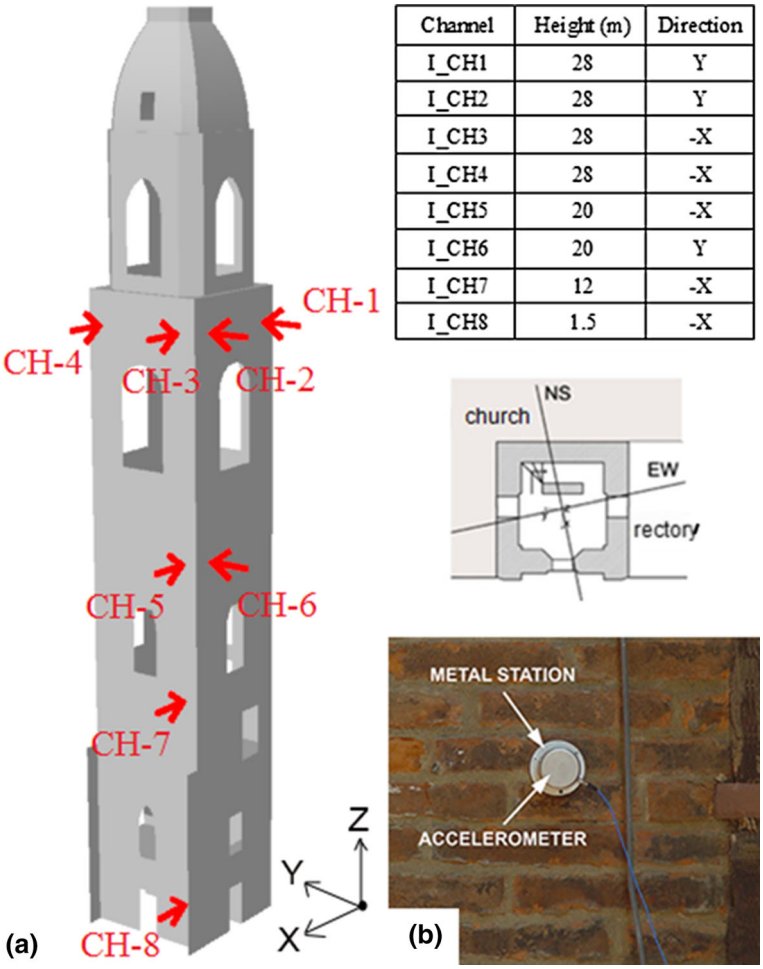


Fig. 5 Post-earthquake provisional safety-interventions: metal tie rods (*1*), wooden falsework in the small opening of the first and second level (*2*, *4*), wooden falsework in the large opening of the third level (*3*)

The accelerometers were installed by means of special metal bases fixed directly on the wall with expansion anchors (Fig. 6b). The metal bases were left in place to simplify the execution of more tests to assess further damage and the long-term effectiveness of the



Channel	Height (m)	Direction
I_CH1	28	Y
I_CH2	28	Y
I_CH3	28	-X
I_CH4	28	-X
I_CH5	20	-X
I_CH6	20	Y
I_CH7	12	-X
I_CH8	1.5	-X

Fig. 6 **a** Instrumentation setup, location and orientation of accelerometers. **b** Detail of the installation of the accelerometer on the bell-tower

safety interventions. A total of 8 channels were acquired with a sampling frequency of 192 Hz, for an average signal length of 300 s. The setup was designed to capture the first main modes of the bell-tower (Boscato et al. 2016). Pre-processing and data conditioning involved subsampling (sampling frequency was reduced to 48 Hz), mean removal and detrending through a polynomial fitting of the signals (Ceravolo et al. 2016). The acquisition of the signals was conducted in similar environmental conditions, with a temperature of about 20 °C and 40 % of humidity.

3.2 Dynamic identification procedure

Table 1 shows the modal parameters identified before (PR-I) and after (PS-I) the implementation of the safety interventions. System identification was carried out in the time domain, using the Stochastic Subspace Identification (SSI) algorithm, with the so-called

"Canonical Variate Analysis" (Van Overschee and De Moor 1996). The output only SSI implementation identifies systems by assuming input excitation as white Gaussian noise. This assumption is commonly accepted in ambient vibrations testing and it was respected during the test phases, being the absence of external excitation sources like machineries or occupants. Signal intervals affected by occasional spikes or anomalous vibration levels have been discarded from analyses. The subspace algorithm identifies the matrix describing the linear system starting from subspaces containing the projections of data matrices. In particular, these types of algorithms project the space of the matrix rows of future outputs into the space of the rows of past outputs.

Figure 7 shows the stabilisation diagrams obtained for some of the signals made available by dynamic monitoring. The identification procedure entails a series of pre-processing operations on the signals (mean removal, de-trending, filtering) carried out by an expert operator in order to ease the identification process of the algorithm. For a detailed discussion on the identification process for masonry structures one can refer to Ceravolo et al. (2016).

From the modal frequencies and from Δf it can be clearly noticed how the installation of the safety interventions mitigated the effects of the extensive damage suffered by the bell-tower (De Stefano and Ceravolo 2007). In fact, the first two bending modes (Table 1) increased of the 16 and 21 %, from 0.68 and 0.72 to 0.79 and 0.87 Hz; whereas the first torsional mode had an increase of 32 %, from 1.41 to 1.86 Hz. For what concerns the damping ratios, the trend is not as clear. Anyhow, 6 out of the 8 modes listed in Table 1 show an increase in the damping ratios after the interventions.

In order to clarify the significance of these results, a comparison is made with another bell-tower where dynamic identifications were carried out before and after the safety interventions. Extensive dynamic campaigns were performed on the S. Annunziata in Roccaverano bell-tower (De Stefano and Ceravolo 2007) before and after a strengthening intervention with grouting and tie-bars. In that case, the bending modes rose from 1.66 and 2.26 to 1.97 and 2.34 Hz, showing an increase of 19 and 4 %, respectively. On the other hand, the torsional mode had an 8 % reduction, from 4.67 to 4.3 Hz.

The first three modes of the bell tower were then compared with those of about 40 masonry towers or bell towers from across Europe. This highlighted how the two flexural modal frequencies of the damaged scenario are significantly lower than the typical ones of other bell-towers of comparable height. From these same data it can be inferred that the torsional mode is even more distant from the "ideal" trend of frequency as a function of

Table 1 Identified modal frequencies and damping ratios in Pre- (PR-I) and post-safety intervention (PS-I) configurations

PR-I		PS-I		Δf (%)	$\Delta\zeta$ (%)
Frequency (Hz)	Damping ratio (%)	Frequency (Hz)	Damping ratio (%)		
0.68	1.6	0.79	1.7	16.2	6.2
0.72	1.5	0.87	0.5	20.8	−66.7
1.41	2.2	1.86	2.6	31.9	18.2
2.30	1.1	2.48	2.3	7.8	109.1
2.71	1.9	3.05	2.2	12.5	15.8
3.68	4.4	4.66	3.1	26.6	−29.5
3.86	0.9	5.48	3.5	42.0	288.9
3.92	0.9	6.26	2.2	59.7	144.4

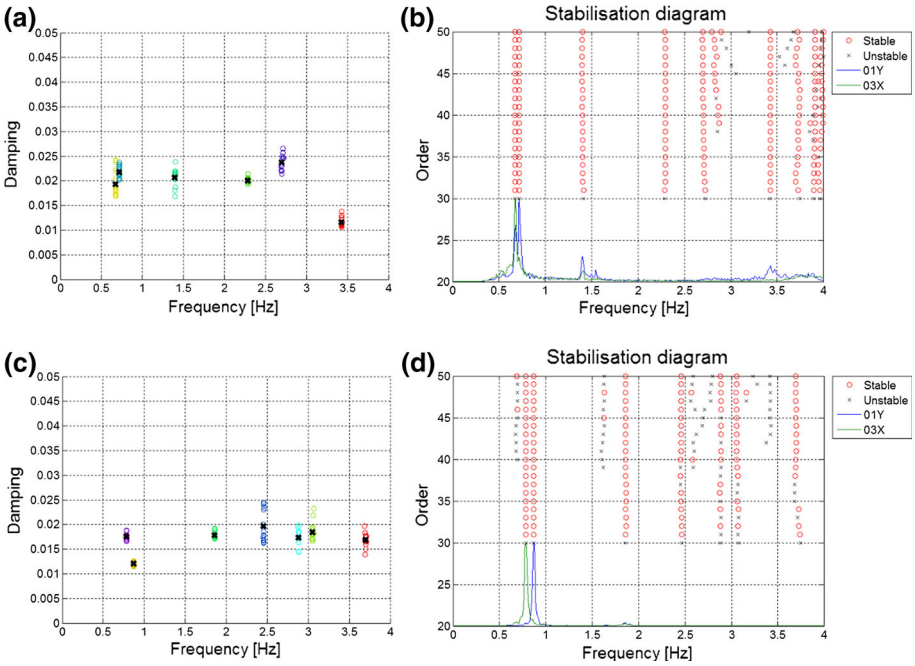


Fig. 7 Bell-tower modal identification results (frequency-damping clustering and stabilisation diagram): **a**, **b** PR-I, **c**, **d** PS-I. The stabilisation parameters chosen for the graph were: $\delta f = 0.005$, $\delta\zeta = 0.1$, MAC = 0.95

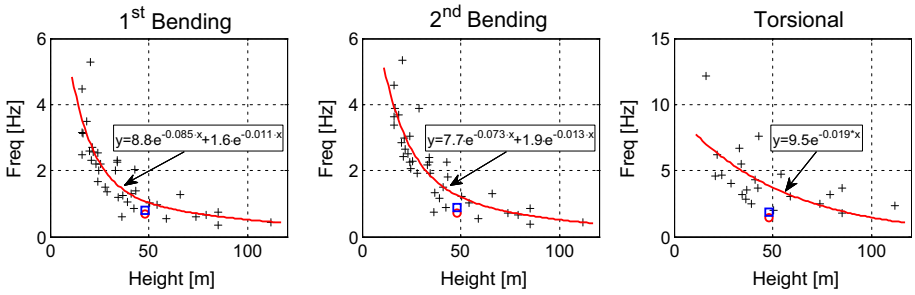


Fig. 8 Frequency dependency of the first 2 bending and the torsional mode with respect to height of the building from literature data. The *red circle* and the *blue square* represents the Mirandola bell-tower frequencies in the PR-I and PS-I configuration respectively, whilst the *regression line* is obtained with a generic exponential law

height represented by the lines in Fig. 8. This is most probably a symptom of a severely damaged structure, where box-like behaviour has been strongly affected. In fact, stiffness along the plane of the masonry walls is relatively less affected by the presence of cracks than torsional stiffness, which is influenced by the state of the connections between orthogonal wall panels. The full list of bell tower modes, up to the sixth, can be found in Table 2.

Table 2 Comparative study of various experimental frequency identified on undamaged masonry towers and bell tower across Europe

	Building	Height (m)	Frequency (Hz)					
			1st	2nd	3rd	4th	5th	6th
Foti et al. (2012a)	Maddalena Church, Bari	16	4.46[b]	4.58[b]	12.16[t]			
Lund et al. (1995)	St Michael's Heighington	16.2	3.16[b]	3.63[b]				
Lund et al. (1995)	Christchurch Consett	16.3	2.48[b]	3.38[b]				
Lund et al. (1995)	St Margaret's Tanfield	16.5	3.13[b]	3.88[b]				
Lund et al. (1995)	St John's Shildon	18.5	3.49[b]	3.68[b]				
Lund et al. (1995)	St Brandon's Brancepeth	20	2.59[b]	2.84[b]				
Ramos et al. (2010)	Clock Tower, Mogadouro	20.4	2.15[b]	2.58[b]	4.98[t]	5.74	6.76	7.69
Lund et al. (1995)	St Andrew's Roker	20.5	5.28[b]	5.34[b]				
Foti et al. (2012b)	Administration Building, Bari	21	2.30[b]	2.43[b]	4.19[b]	4.60[t]	5.02[b]	
Lund et al. (1995)	St Michael's Houghton	21.4	2.71[b]	2.98[b]				
Bayraktar et al. (2009)	Hagia Sofia, Trabzon	22	2.56[b]	2.65[b]	6.22[t]			
Lund et al. (1995)	St Andrew's B. Auckland	23.2	2.20[b]	2.51[b]				
Bonato et al. (2000)	S Annunziata, Roccaverano	24	1.66[b]	2.26[b]	4.67[t]	6.18[b]	6.40[t]	8.90[b]
Lund et al. (1995)	St Mary's Richmond	24	2.55[b]	3.04[b]				
Lund et al. (1995)	St Oswald's, Durham	24.8	2.01[b]	2.05[b]				
Lund et al. (1995)	St Edmund's Sedgefield	25.4	2.20[b]	2.28[b]				
Lund et al. (1995)	St Matthew's Newcastle	28	1.49[b]	1.92[b]				
Abruzzese (2005)	Capocci Tower, Rome	33.1	2.00[b]	2.17[b]	6.70[t]	8.52[b]	9.01[b]	
Lund et al. (1995)	St Cuthbert's Benfieldside	33.8	2.25[b]	2.27[b]				
Orihuela-spain et al. (2008)	Santa Justa y Rufina	33.9	2.30[b]	2.40[b]	5.50[t]			
Júlio et al. (2008)	Tower of the University, Coimbra	34	2.13[b]	2.47[b]	6.55[t]	8.25[b]	9.71[b]	
Bennati et al. (2005)	Tower of Matilde, S. Miniato	34.3	1.20[b]	1.91[b]	3.22[t]	5.98[b]	7.055[b]	8.31[t]
Russo et al. (2010)	St Andrea, Venice	36.2	0.61[b]	0.73[b]	2.81[t]	3.54[b]	5.39	
Gentile et al. (2012)	Arcisate bell tower	36.72	1.25[b]	1.32[b]	3.52[t]	4.06[b]	4.25[b]	
Casciati and Al-Saleh (2010)	Soncino Civic Tower	39.24	1.05[b]	1.15[b]	2.50[t]	4.10[b]	4.30[b]	
Ivorra and Pallarés (2006)	Nuestra Sra Misericordia, Valencia	41	1.29[b]	1.49[b]	3.98[t]	4.32[b]	4.37[b]	
Ivorra et al. (2009)	San Nicolas, Valencia	42.5	0.85[b]	0.87[b]	3.69[t]			

Table 2 continued

	Building	Height (m)	Frequency (Hz)					
			1st	2nd	3rd	4th	5th	6th
Diaferio et al. (2014)	Cathedral Trani, Trani	43	2.04[b]	2.26[b]	7.03[b]	7.60[t]	9.16[b]	
Lund et al. (1995)	St Nicholas', Durham	43.5	1.38[b]	1.82[b]				
Ceravolo et al. (2016)	S. Giovenale, Fossano	46	1.29[b]	1.34[b]	3.28[t]	4.11[b]	4.74[b]	6.65[t]
Cunha et al. (2014)	Clerigos Tower, Porto	50.6	1.02[b]	1.21[b]	1.99[b]	2.84[t]	3.19[b]	
Saisi and Gentile (2015)	Gabbia Tower, Mantua	54	0.98[b]	1.03[b]	3.891[b]	4.763[t]	6.925[b]	
Ceroni et al. (2009)	St Maria del Carmine, Naples	58	0.69[b]	0.76[b]	2.28[b]	2.35[b]	2.76[t]	
Bassoli et al. (2015)	St Antonio, Ficarolo	59	0.55[b]	0.56[b]	2.16[b]	2.17[b]	3.07[t]	6.24[b]
Lund et al. (1995)	Cathedral Durham	66	1.28[b]	1.31[b]				
Gentile and Saisi (2007)	Monza Cathedral (P-I)	74	0.59[b]	0.71[b]	2.46[t]	2.73[b]	5.71[b]	
Modena et al. (2002)	Monza Cathedral (PS-I)	74	0.65[b]	0.66[b]	3.18[t]	3.23[b]	3.31[b]	5.71[t]
Pieraccini et al. (2014)	Torre del Mangia, Siena	85	0.35[b]	0.39[b]	1.8[b]	1.91[b]		
Sabia et al. (2015)	Ghirlandina Tower, Modena	85	0.74[b]	0.85[b]	2.77[b]	2.99[b]	3.66[t]	4.81[b]
Binda et al. (2000)	Torrazzo Cremona	112	0.44[b]	0.44[b]	1.66[b]	1.66	2.36	2.81[b]

[b] Bending modes, [t] torsional modes

It is also worth noting that, in the PR-I condition, the first and the second flexural modal shapes, directed along E–W and N–S directions respectively, show a coupled behaviour and a value of Modal Assurance Criterion (MAC) of 0.495, whereas after the strengthening interventions they appear almost perfectly aligned with the principal axes of the tower, the MAC decreases to 0.001 (Fig. 9).

4 FE model calibration

A finite element (FE) model was built using Ansys code on the basis of the information gathered with both geometric surveys and historical documentation, and then calibrated by using the experimental results. The geometric model was created according to both historical data and a laser scanner survey. The masonry panels composing the bell-tower were idealised as plane and curved surfaces. This led to the use of shell-type finite elements to discretise the geometric model. FEs were successively grouped in sub-parts defined in terms of historical, structural and typological homogeneity (Ceravolo et al. 2014; Boscato et al. 2015). In total, five different sub-parts were individuated, at different levels of the bell-tower (Fig. 10). The first and the second sub-parts are the basement and the following upper level which were both built in the late fifteenth century. The masonry vaults belonging to the basement level were also modelled by shell-type finite elements,

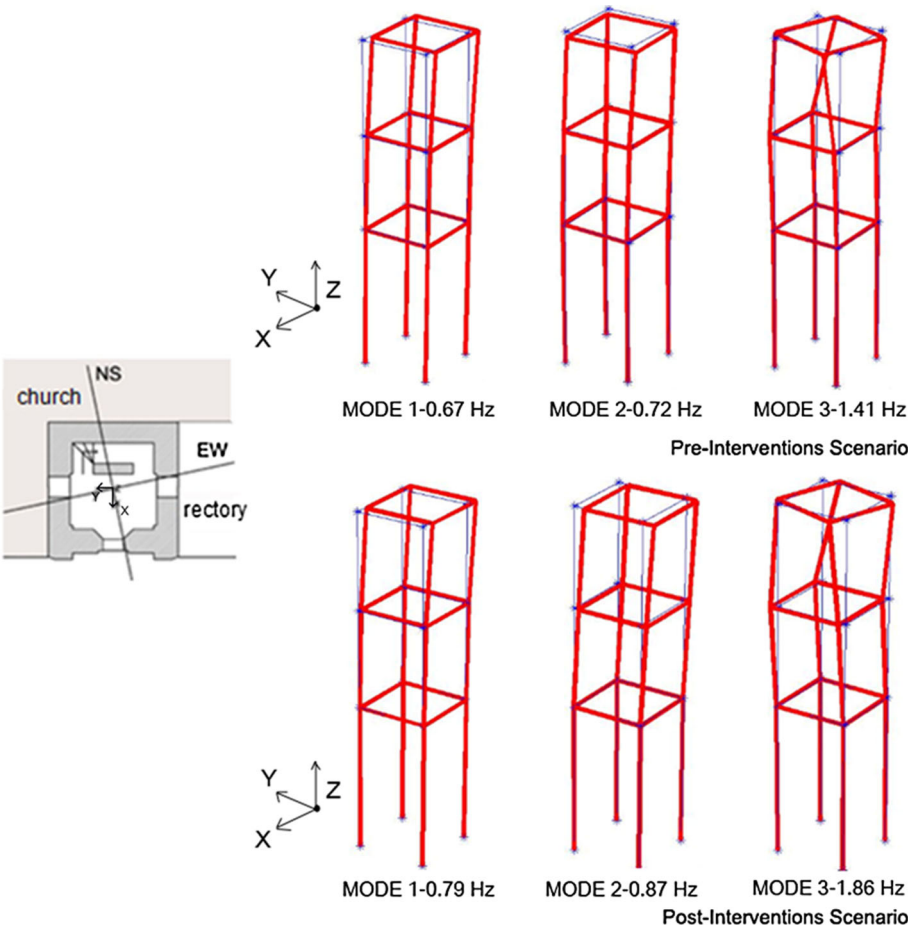


Fig. 9 Bell-tower identified frequencies and modal shapes in the PR-I scenario and the PS-I scenario

attributing a modified equivalent density property in order to take into account the inertial contribution of the staircase and the slabs. The third sub-part roughly corresponds to the 1st belfry, built in the eighteenth century, and it is characterised by its large openings. The last two levels are the 2nd belfry, rebuilt in 1888, and the stone roof of the belfry.

The initial properties of the masonry were assumed from the literature (Fernandes et al. 2010) and from the current Italian code (i.e. Young modulus: 1.5 GPa, Poisson's ratio: 0.4, density: 1900 kg/m^3). A second type of material (Young modulus: 1.5 GPa, Poisson's ratio: 0.4, density: 1700 kg/m^3) was attributed to the shell elements of the stone dome. In the baseline FE model, a thickness of 1.15 m was set for the two first levels according to the available data, whilst thickness of 0.55 and 0.35 m were assigned to the other two sub-part levels according to the visual inspection.

For the boundary conditions of the tower, and specifically its interactions with the adjacent buildings (i.e. the Cathedral of Santa Maria Maggiore and the rectory), linear spring elements were used on each side (East, West and North) in correspondence to the rectory wall, the apse arches and the nave walls, as it is possible to notice in Fig. 11. In the

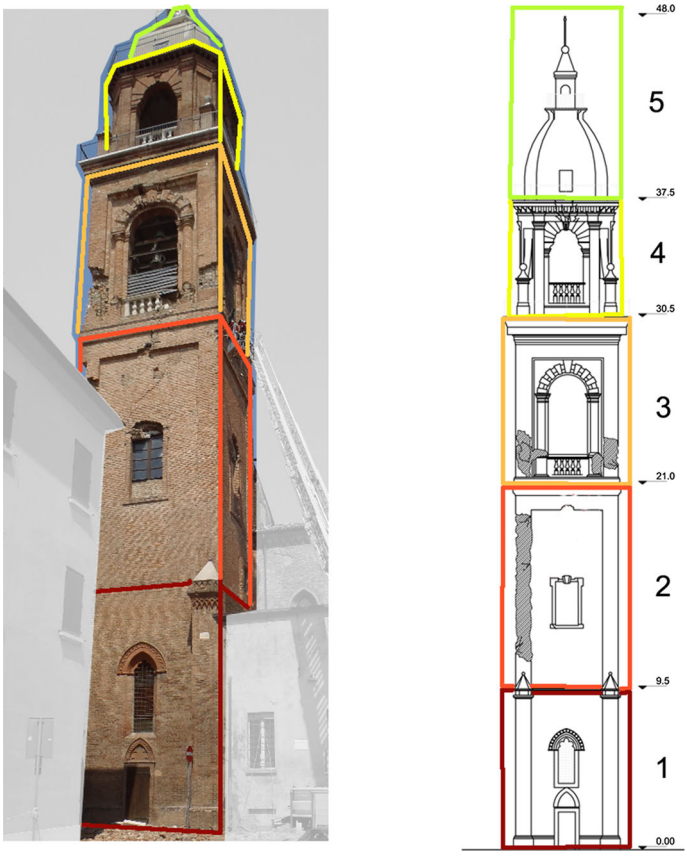


Fig. 10 The five sub-parts of the bell-tower

baseline FE model, the stiffness coefficient was set to 1×10^{11} N/m for all the spring elements. Concerning the foundations, it was chosen not to model them and to assume the structure as fixed at its base. This assumption was made according to the decision of avoiding the investigation of rocking motion in the dynamic behaviour of the tower that commonly occurred in slender structures (Sabia et al. 2015). In fact, the monitoring setup was not specifically designed to detect rocking motion in the structure, and these effects can be assumed negligible in case of low vibration levels, as recorded during the ambient vibration testing.

In a second phase, the safety interventions were added to the FE model (Fig. 12b). The interventions were modelled resorting to beam and truss type finite elements idealising the wooden falsework installed in the openings of the bell-tower at the different levels (Fig. 5). The material properties (Young modulus: 8 GPa, Shear Modulus: 0.5 GPa, density 370 kg/m^3) assigned to these elements were chosen according to the Italian Fire Department's manual for safety wooden interventions (Ministero dell'Interno and Corpo Nazionale dei Vigili del Fuoco 2011). The metal tie-rods were not modelled with specific finite elements, but the effect of their presence is evaluated indirectly during the model updating phase by the variation of the mechanical properties. If the intervention is effective, the metal tie-rods

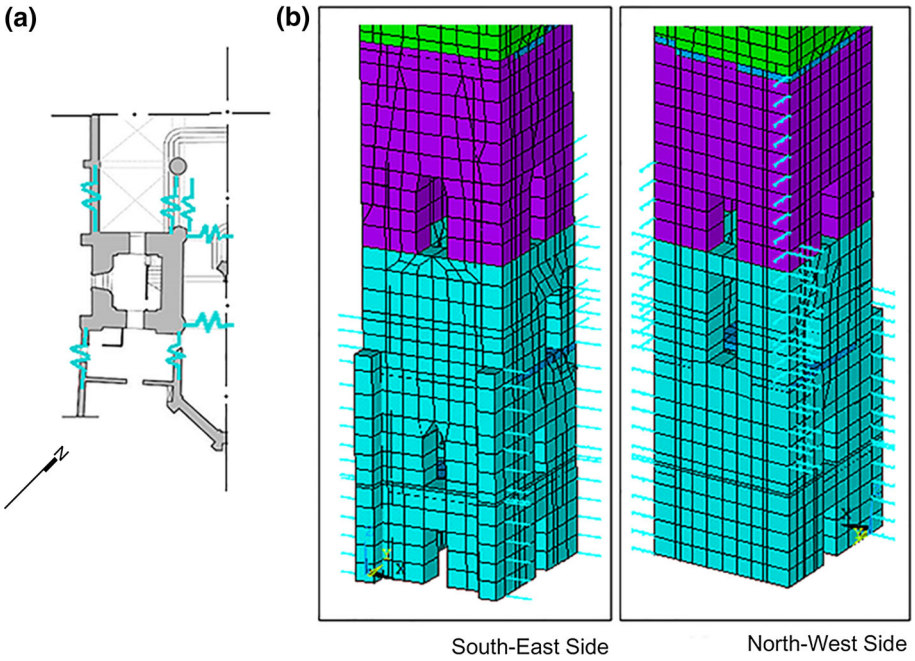


Fig. 11 **a** Idealisation of spring elements as boundary conditions due to nearby buildings. **b** Localization of the 3D-linear spring elements on the FE model

should lead to a partial closure of the cracks and to the rehabilitation of the original box-like behaviour of the structure. Thus, the efficacy of the intervention can be inferred by the equivalent stiffness increase of the respective sub-part.

4.1 Model updating

Model updating is nowadays a common procedure for damage evaluation or assessment of cultural heritage and, more specifically, of masonry structures (Ceravolo et al. 2016). The intrinsic difficulties in the procedure (e.g. heterogeneity of the material, uncertainty in boundary conditions) are overshadowed by the advantage of being able to monitor and tune the model with global indicators of the physical system. Although this type of approach may lead to higher uncertainties for local values of physical quantities, it minimises the uncertainties of the overall system response.

The experimental modal quantities listed in Table 1 have been used to calibrate the baseline FE model, resorting to an indirect method of model updating (Friswell and Mottershead 1995). Indeed, the updating procedure consists in the minimisation of a penalty function which correlates the updating parameter vector (**p**), the i-th numerical frequency ($f_{ID,i}$),the i-th experimental frequency ($f_{FEM,i}$) and the Modal Assurance Criterion (MAC_i) between the i-th identified mode-shape and the corresponding i-th analytical mode-shape. The α and β terms are the weight factors for the frequency and the mode-shape errors, respectively (in the described application both were set equal to 0.5).

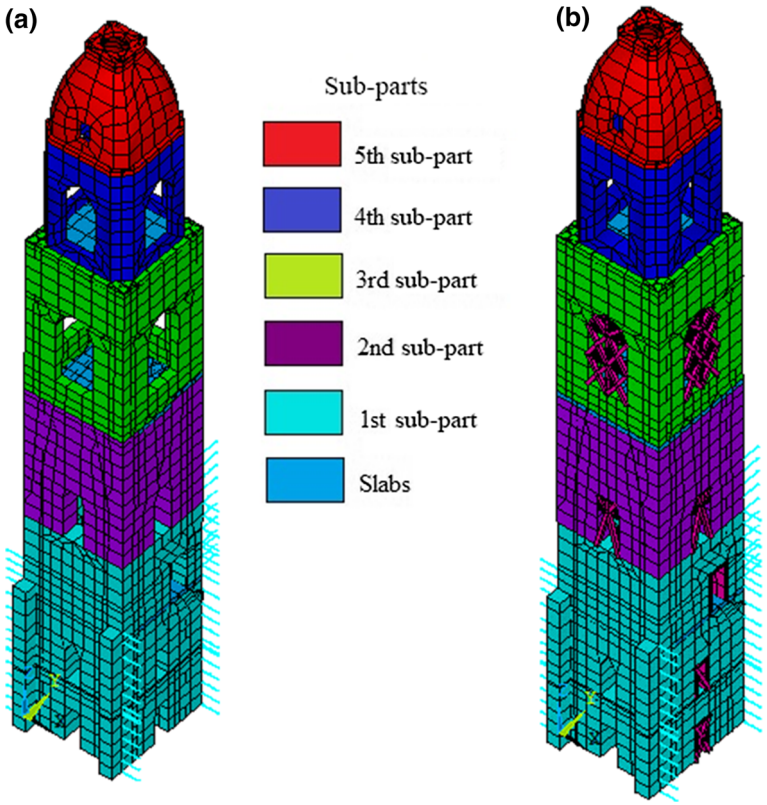
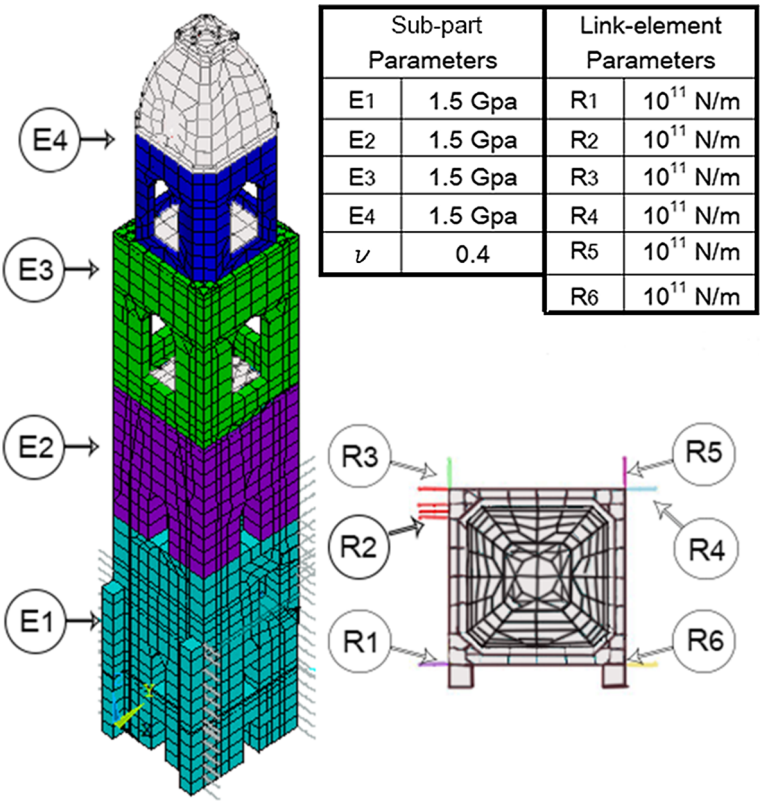


Fig. 12 Baseline FE model of the bell-tower subdivided in sub-parts (**a**), FE model with safety interventions (**b**)

$$\varepsilon(\mathbf{p}) = \sum_{i=1}^{m} \left[\alpha_i \left(\frac{f_{ID,i} - f_{FEM,i}}{f_{ID,i}} \right)^2 + \beta_i \frac{\left(1 - \sqrt{MAC_i}\right)^2}{MAC_i} \right] \tag{1}$$

The parameters selected for the updating process are the Young modulus and the Poisson's ratio for the sub-parts 1–4. Parameters have been chosen on the basis of a previously sensitivity analysis on the model, in order to discriminate among the most significant parameters to be updated. For instance, for what concerns the sub-part number 5, since no sensors were placed at that level, the sensitivity of the penalty function with respect to the parameter of this sub-part is too low to be considered for updating. Moreover, the 6 link-elements stiffness were updated for a total of 11 updating parameters (Fig. 13). It is worth to remark that at this stage it is unknown the level of connection existing between the bell tower and the body of the church.

In Table 3 the comparison between the analytical and the experimental modal parameters can be appreciated in terms of both frequency and MAC in the pre-intervention scenario. The MAC value between analytical and identified modal shapes is greater than 0.8 for 3 modes out of 6. Firstly, the parameters of the connection with the adjacent buildings were updated, thus assessing the conditions of restraint of the bell tower. From the obtained values, the most influential connections are those with the nave of the church



Sub-part Parameters		Link-element Parameters	
E1	1.5 Gpa	R1	10^{11} N/m
E2	1.5 Gpa	R2	10^{11} N/m
E3	1.5 Gpa	R3	10^{11} N/m
E4	1.5 Gpa	R4	10^{11} N/m
ν	0.4	R5	10^{11} N/m
		R6	10^{11} N/m

Fig. 13 Finite element model discretization associated to the chosen updating parameters and related initial values

on the North side, whilst the parameters related to the arches of the nave and apse have values definitely lower. This is probably due to the collapse of the roof of the church, the absence of connection between the walls of the nave reduces its constraint action for the bell-tower. A first rough manual tuning of the masonry density and the Poisson's ratio and also the thickness of the third and fourth level was carried out with respect to the first three natural frequencies. Then, the updating process was performed for the Young's modulus parameter of the four masonry levels starting from the initial values of 1.5 GPa.

The results of the updating procedure provide further information about the bell-tower damage state (Fig. 14b): the value of 0.508 GPa for the Young modulus of the first sub-part and the others of the upper levels, 0.806 GPa for the second level and 0.85 GPa for the third one, refer to heavily cracked regions of the building. Moreover, these results suggest that the first sector is strongly influenced by adjacent bodies, that have stiffened the basement of the tower, especially on the west side, where the spring-element $R_1 = 4.13 \times 10^6$ N/m represent the external wall of the church's nave; and on the east-side where $R_5 = 1.5 \times 10^9$ N/m, $R_4 = 6.34 \times 10^5$ N/m, $R_6 = 106{,}250$ N/m model the rectory building.

The results of the updating in terms of frequency errors and MAC for the PS-I are listed in Table 4: the frequency errors are slightly higher in this case but the MAC values

Table 3 Comparison between the analytical and the experimental modal model of bell-tower in pre-intervention condition

Mode	Frequency ID (Hz)	Frequency FEM (Hz)	Err (%)	MAC
1	0.68	0.68	0.2	0.98
2	0.72	0.69	3.8	0.98
3	1.41	1.73	18.3	0.91
4	2.29	2.33	1.6	0.68
5	2.70	2.42	11.8	0.66
6	3.68	3.80	3.3	0.35

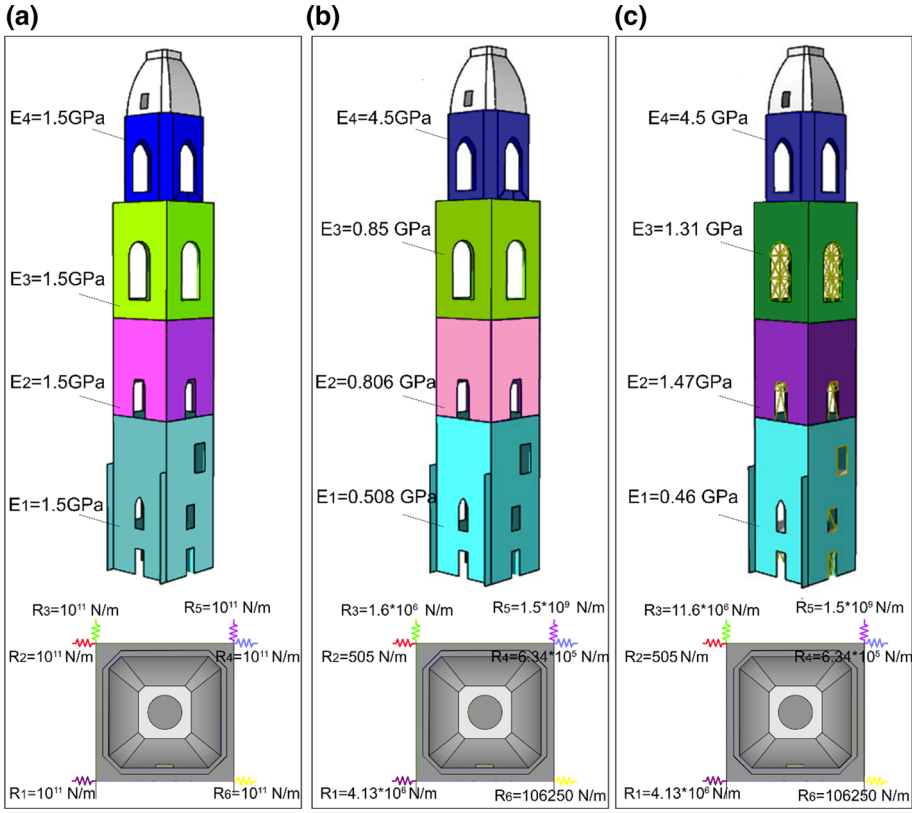


Fig. 14 Model updating results: initial values (**a**) and the updated values for the pre-intervention scenario (**b**) and in the post-intervention scenario (**c**)

confirmed a good match between the numerical model and the experimental data. Also in this second case, 3 modes have a MAC value higher than 0.9 (Table 4).

The second updating procedure (on the PS-I model) was carried out by varying only the values of Young's modulus of the masonry (E_1, E_2, E_3, E_4). The parameters related to the adjacent bodies are set equal for both conditions as the configuration is assumed to be unchanged: in fact, the safety interventions should affect the bell tower but not the

Table 4 Comparison between the analytical and the experimental modal model of bell-tower in post-intervention condition

Mode	Frequency ID (Hz)	Frequency FEM (Hz)	Δf (%)	MAC
1	0.79	0.71	11	0.97
2	0.87	0.75	16	0.97
3	1.86	2.03	8	0.96
4	2.48	2.85	13	0.85
5	3.05	3.05	0	0.68
6	4.66	4.66	0	0.28

connection with the surrounding buildings. The first sub-part, where there are only the wooden false works in correspondence of the opening, does not show any significant variation in the Young's modulus parameter. On the other hand, the second sub-part is the most influenced by the safety interventions (tie-rods are located on this level), the related Young's modulus parameter has a significant increase from the value of 0.805–1.47 GPa (parameter E_2, Fig. 14c). The third sub-part, also affected by the installation of tie rods, reveals a relevant increase of stiffness with a Young's modulus value of 1.31 GPa respect the starting updated value of the pre-intervention scenario (parameter E_3, Fig. 14c). These results highlight how the equivalent stiffness is modified in correspondence of the areas that underwent more invasive interventions. Therefore, the updated model has been a valid support to confirm the experimental model and measurements, and also to plan any additional tests on the bell-tower.

4.2 Dynamic response to aftershock events

In a post-earthquake scenario, the evaluation of the structural safety is a challenging task, since a decision has to be made in the shortest time possible. Thus, complicated non-linear FE models, where the nonlinear laws of the materials requires the initialisation of several parameters, may not always be the best answer for a timely response. The use of linear-elastic models may be of some use in order to roughly assess the dynamic behaviour of the building. The approach proposed in this paragraph is a quick but reliable assessment of the dynamic behaviour of the Mirandola bell tower using the linear but calibrated model. It has been seen from the previous paragraph that a dependency between frequency and PS-I state may be inferred from the results. Consequently, the updated FE model may be used in order to investigate the structural response considering just the linear dynamic behaviour of the structure. Different time-history analyses have been carried out, in order to compare the seismic responses of the two tuned FE models (in the pre- and post-earthquake safety intervention configurations) in terms of displacements using three aftershocks accelerograms (referring to the 20–21 May event). The three main events with aftershocks were recorded by the same station in Mirandola (MRN), which is part of the Italian accelerometric network (ITACA). Table 5 lists the aftershock events, with their respective magnitudes and peak ground accelerations (PGA).

Figure 15 shows the aftershock accelerograms used as input for the dynamic analysis and their frequency content. For brevity's sake, only the accelerograms referring to the main direction of the earthquake are reported (which are respectively N–S for the first two and E–W for the third one) but a three component excitation has been applied to the FE model.

Table 5 Aftershock events, related Magnitude and PGA

Date and time	Label	Magnitude	PGA (g)	Depth (km)	Epicentral distance (km)
29/05/2012 11:00:22 (UTC)	AS1	5.4	0.204	5.4	10
03/06/2012 19:20:33 (UTC)	AS2	5.1	0.175	9.2	5.1
12/06/2012 01:48:26 (UTC)	AS3	4.3	0.064	10.8	14.6

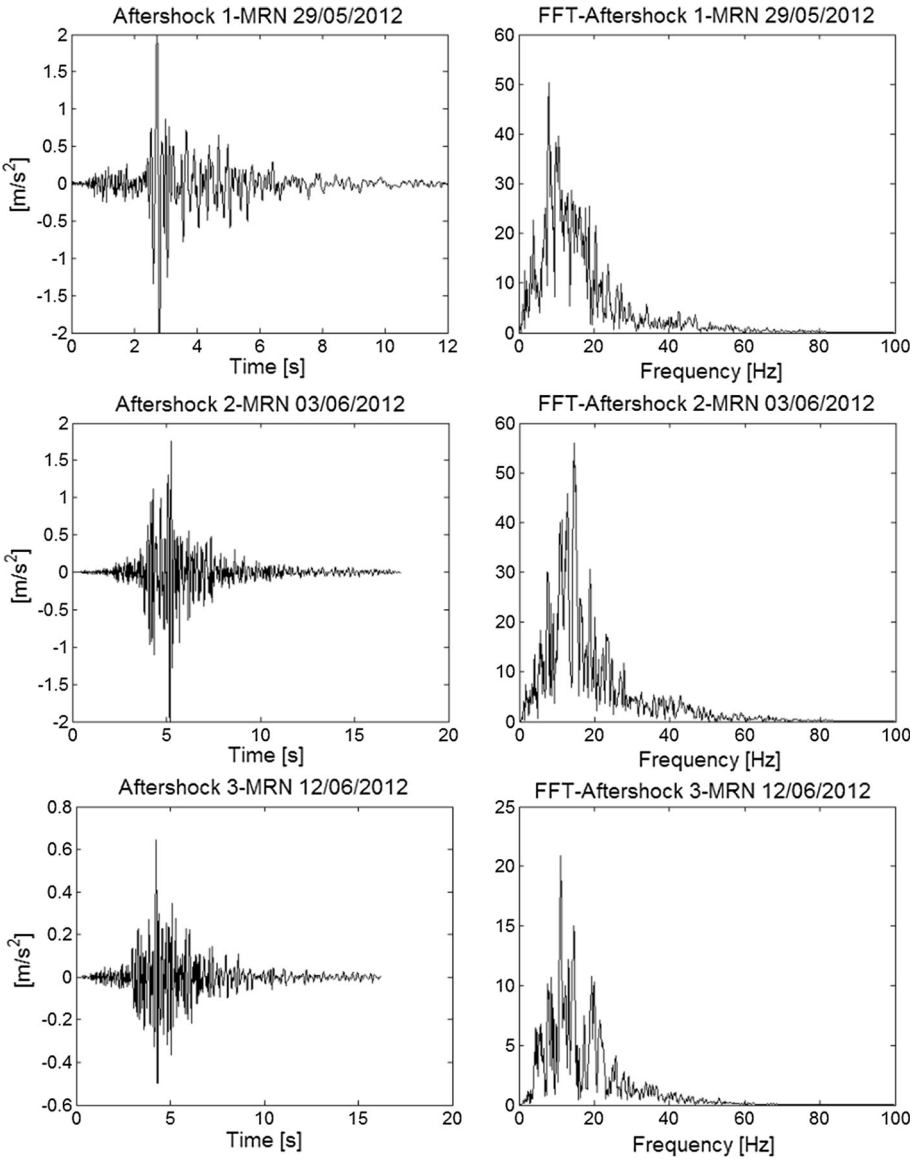


Fig. 15 Acceleration and frequency response spectra of the three aftershocks related to the respective main direction

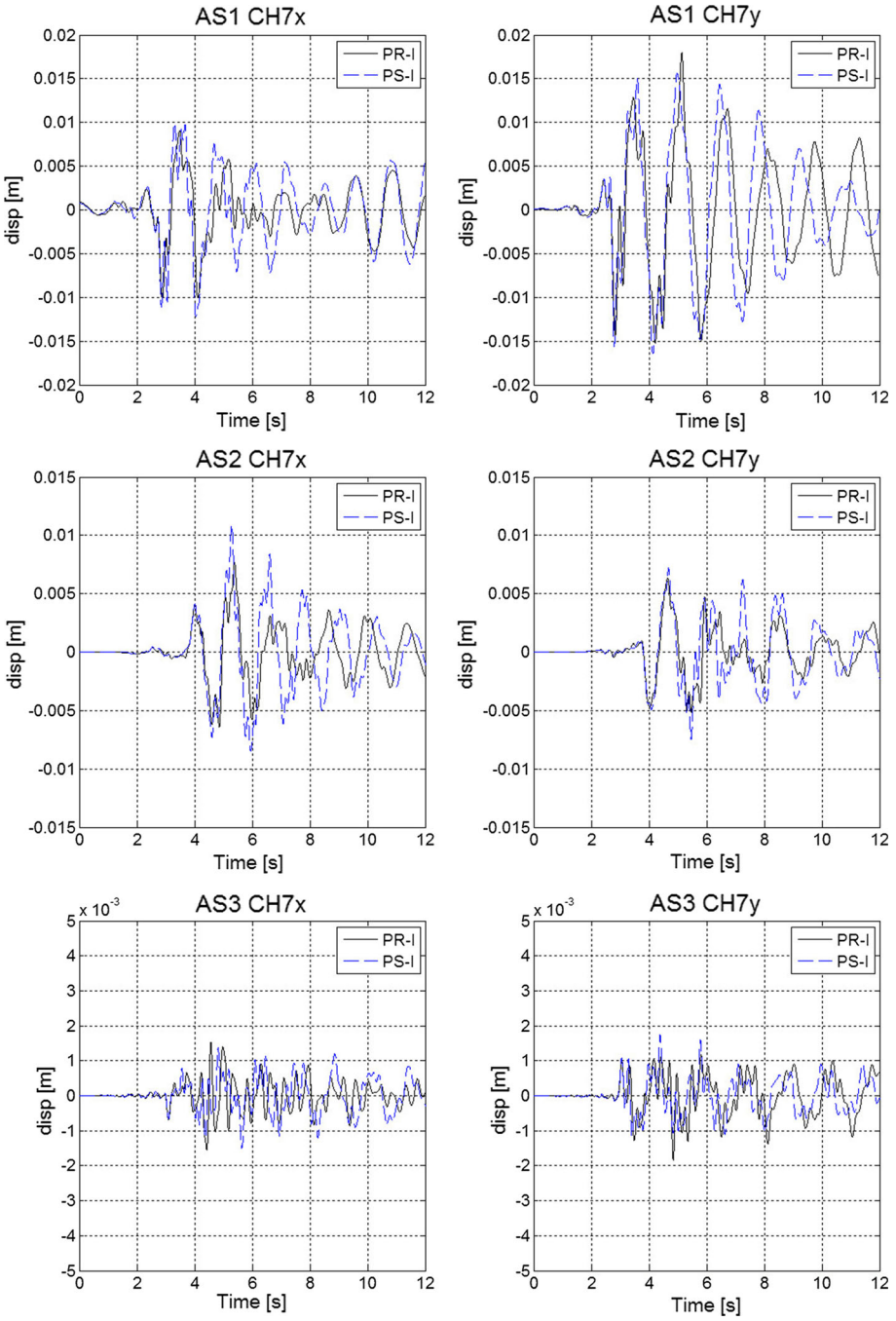


Fig. 16 Comparison between the displacement responses related to CH7-position (direction *x*—first column, direction *y*—second column) in the pre (*red line*) and post (*blue line*) condition

Table 6 Comparison of the dynamic response of the bell-tower to the accelerograms of Fig. 15 in terms of maximum displacement in the PR-I and PS-I configurations

Disp (mm)	AS1			AS2			AS3		
	PR-I	PS-I	Δ (%)	PR-I	PS-I	Δ (%)	PR-I	PS-I	Δ (%)
CH7-x	11.30	12.20	8.0	7.70	10.90	41.6	1.50	1.50	0.0
CH7-y	22.60	16.40	−27.4	6.30	7.40	17.5	1.80	1.70	−5.6
CH3-x	2.30	3.80	65.2	1.70	4.10	141.2	0.75	0.99	32.3
CH3-y	5.20	6.00	15.4	2.30	3.80	65.2	0.65	0.97	49.4

Finally, the results of two points (roughly corresponding to CH-3 and CH-7 in Fig. 6) carefully chosen in the structure, respectively at 12 and 28 m of height were used as a benchmark of comparison for the PR-I and PS-I configurations. Both points should be affected by the false works at the openings and the safety interventions, and the updating results seemed to confirm this effect, because the elastic modulus in correspondence of the 2nd and 3rd sub-part showed a sensible variation.

The maximum displacements values are obtained for the CH-7 position, located in a higher, thus more flexible region of the tower, where the most severe damages were assessed (see Fig. 2). Observing the time-history responses in Fig. 16 and the results in Table 6 it is possible to notice how the amplitude of the response in the PR-I and PS-I configurations is quite similar with all the three aftershocks. As shown in Fig. 16, the response in the direction of the x and y reveals quite similar results between PR-I and PS-I differing only by the time of occurrence of the peak displacement. Only the responses to AS1 and AS3 aftershocks show an improvement of global behaviour when considering the maximum response in terms of displacement.

5 Conclusions

This work has presented the results of an experimental dynamic campaign carried out on the bell-tower of S. Maria Maggiore in Mirandola, struck by the 2012 Emilia earthquake. Data were acquired in two distinct phases: one immediately after the seismic event, with extensive damage on the structure, and the second one after the realisation of the provisional safety interventions. This allowed for a comparison of the dynamic behaviour of the structure in a pre- and post-intervention scenario. A series of considerations can be drawn.

1. Comparing the results, a general increase in terms of modal frequencies is observed, which can be directly related to the stiffening effects provided by the safety interventions realised. For what concerns the damping ratios, the modes in direction X and the torsional ones show an increase of the equivalent viscous damping, whilst the flexural modes in direction Y show a decrease in the damping after the interventions.
2. A comparison between the case study and literature bell-towers highlights how after the seismic event the frequencies of the first three modes were found to be sensibly low. After the strengthening intervention frequency values are seen to substantially match those expected for undamaged bell-towers of similar height.

3. Vibration-based monitoring allows to calibrate a FE model that can be potentially used for assessing the intrinsic characteristics of masonry, the structural interaction with adjacent buildings and the structural effects of safety measures and strengthening interventions. It is worth to add that a set of dynamic test on the pristine (or pre-earthquake) state of the structure may strongly improve the quality of the results obtained.
4. The model updating procedure allowed a significant number of parameters of the different structural portions to be calibrated, as required in the analysis of complex structures.
5. The observed increase in modal frequency values proves that the confinement provided by safety measures limits the flexural mechanism; the increase of Young modulus in the portion of structure interested by post-earthquake measures implies the increment of global flexural stiffness.

In conclusion, the model updating procedure confirmed to be an effective tool for investigating the behaviour of structures in complex scenarios. Moreover, results show how the presence of a dynamic monitoring system in the aftermath of a seismic event can be helpful to assess the residual structural performances, the degradation of mechanical characteristics and the effectiveness of safety interventions immediately after their installation and over time, up to the retrofitting of the structure.

Acknowledgments The authors would like to thank the Laboratory of Strength of Materials (LabSCo) of IUAV University of Venice for their support during the installation and monitoring phases. This research has been conducted within the framework of the multidisciplinary PhD program in Cultural Heritage of the Politecnico di Torino.

Open Access This article is distributed under the terms of the Creative Commons Attribution 4.0 International License (http://creativecommons.org/licenses/by/4.0/), which permits unrestricted use, distribution, and reproduction in any medium, provided you give appropriate credit to the original author(s) and the source, provide a link to the Creative Commons license, and indicate if changes were made.

References

Abruzzese D (2005) Seismic resistance of masonry towers. In: Proceedings of the 4th international seminar on structural analysis of historical constructions, pp 451–460

Bassoli E, Vincenzi L, Bovo M, Mazzotti C (2015) Dynamic identification of an ancient masonry bell tower using a MEMS-based acquisition system. In: 2015 IEEE Workshop on Environmental, Energy and Structural Monitoring Systems (EESMS), pp 226–231. doi:10.1109/EESMS.2015.7175882

Bayraktar A, Türker T, Sevim B, Altunişik AC, Yildirim F (2009) Modal parameter identification of Hagia Sophia bell-tower via ambient vibration test. J Nondestruct Eval 28:37–47. doi:10.1007/s10921-009-0045-9

Bennati S, Nardini L, Salvatore W (2005) Dynamic behavior of a medieval masonry bell tower. Part II: measurement and Modeling of the Tower Motion. J Struct Eng 131:1647–1655. doi:10.1061/(ASCE)0733-9445(2005)131:11(1647)

Binda L, Falco M, Poggi C, Mirabella Roberti G, Corradi R, Tongini Folli R (2000) Static and dynamic studies on the Torrazzo in Cremona (Italy): the Highest Masonry Bell Tower in Europe. In: International symposium on Bridging Large Spans (BLS) from antiquity to the present. Istanbul, pp 100–110

Bonato P, Ceravolo R, De Stefano A, Molinari F (2000) Cross-time frequency techniques for the identification of masonry buildings. Mech Syst Sign Process 14:91–109. doi:10.1006/mssp.1999.1273

Boscato G, Russo S, Ceravolo R, Zanotti Fragonara L (2015) Global sensitivity-based model updating for heritage structures. Comput Civ Infrastruct Eng 30:620–635. doi:10.1111/mice.12138

Boscato G, Dal Cin A, Ientile S, Russo S (2016) Optimized procedures and strategies for the dynamic monitoring of historical structures. J Civ Struct Heal Monit. doi:10.1007/s13349-016-0164-9

Casciati S, Al-Saleh R (2010) Dynamic behavior of a masonry civic belfry under operational conditions. Acta Mech 215:211–224. doi:10.1007/s00707-010-0343-4
Casciati S, Faravelli L (2010) Vulnerability assessment for medieval civic towers. Struct Infrastruct Eng 6:193–203. doi:10.1080/15732470802664290
Ceravolo R, Pistone G, Zanotti Fragonara L, Massetto S, Abbiati G (2016) Vibration-based monitoring and diagnosis of cultural heritage: a methodological discussion in three examples. Int J Archit Herit. 10:375–395. doi:10.1080/15583058.2013.850554
Ceretti F (1889) Delle chiese dei conventi e delle confraternite della Mirandola. Mirandola
Ceroni F, Pecce M, Voto S, Manfredi G (2009) Historical, architectural, and structural assessment of the Bell Tower of Santa Maria del Carmine. Int J Archit Herit Conserv Anal Restor 3:169–194. doi:10.1080/15583050802347490
Cunha Á, Ramos LF, Magalhães F, Lourenço PB, Engineering F, Frias RR (2014) Dynamic identification and modelling of Clérigos Tower: initial studies. In: Proceedings of the 9th international conference on structural dynamics, EURODYN 2014, pp 1445–1452
De Stefano A, Ceravolo R (2007) Assessing the health state of ancient structures: the role of vibrational tests. J Intell Mater Syst Struct 18:793–807. doi:10.1177/1045389X06074610
Diaferio M, Foti D, Giannocaro NI (2014) Non-destructive characterization and identification of the modal parameters of an old masonry tower. In: 2014 IEEE workshop on environmental, energy, and structural monitoring systems proceedings. IEEE, pp 1–6
Fernandes FM, Lourenço PB, Castro F (2010) Ancient clay bricks: manufacture and properties. In: Dan MB, Přikryl R, Török Á (eds) Materials, technologies and practice in historic heritage structures. Springer, Dordrecht, pp 29–48
Foti D, Chorro SI, Sabbà MF (2012a) Dynamic investigation of an ancient masonry Bell Tower with operational modal analysis a non-destructive experimental technique to obtain the dynamic characteristics of a structure, pp 384–391. doi: 10.2174/1874836801206010384
Foti D, Diaferio M, Giannoccaro NI, Mongelli M (2012b) Ambient vibration testing, dynamic identification and model updating of a historic tower. NDT E Int 47:88–95. doi:10.1016/j.ndteint.2011.11.009
Friswell MI, Mottershead JE (1995) Finite element model updating in structural dynamics. Kluwer, Dordrecht
Gentile C, Saisi A (2007) Ambient vibration testing of historic masonry towers for structural identification and damage assessment. Constr Build Mater 21:1311–1321. doi:10.1016/j.conbuildmat.2006.01.007
Gentile C, Saisi A, Cabboi A (2012) One-year dynamic monitoring of a masonry tower. In: Structural analysis of historical constructions (SAHC 2012). Wroclaw, 15–17 June 2012
Ivorra S, Pallarés FJ (2006) Dynamic investigations on a masonry bell tower. Eng Struct 28:660–667. doi:10.1016/j.engstruct.2005.09.019
Ivorra S, Pallarés FJ, Adam JM (2009) Experimental and numerical results from the seismic study of a Masonry Bell Tower. Adv Struct Eng 12:287–293. doi:10.1260/136943309788251641
Júlio ENBS, da Silva Rebelo CA, Dias-da-Costa DASG (2008) Structural assessment of the tower of the University of Coimbra by modal identification. Eng Struct 30:3468–3477. doi:10.1016/j.engstruct.2008.06.001
Lund JL, Selby AR, Wilson JM (1995) The dynamics of bell towers—a survey in northeast England. Trans Built Environ 15:45–52
Milana G, Bordoni P, Cara F, Di Giulio G, Hailemikael S, Rovelli A (2014) 1D velocity structure of the Po River plain (Northern Italy) assessed by combining strong motion and ambient noise data. Bull Earthq Eng 12:2195–2209. doi:10.1007/s10518-013-9483-y
Ministero dell'Interno, Corpo Nazionale dei Vigili del Fuoco (2011) Manuale Opere Provvisionali L'intervento Tecnico Urgente in Emergenza Sismica
Modena C, Valluzzi MR, Tongini Folli R, Binda L (2002) Design choices and intervention techniques for repairing and strengthening of the Monza cathedral bell-tower. Constr Build Mater 16:385–395. doi:10.1016/S0950-0618(02)00041-7
Orihuela-spain R, Ivorra S, Pallarés F, Adam JM (2008) Experimental and numerical studies on the bell-tower of Santa Justa y. 349–355
Pau A, Vestroni F (2008) Vibration analysis and dynamic characterization of the Colosseum. Struct Control Heal Monit 15:1105–1121. doi:10.1002/stc.253
Pau A, Vestroni F (2013) Vibration assessment and structural monitoring of the Basilica of Maxentius in Rome. Mech Syst Signal Process 41:454–466. doi:10.1016/j.ymssp.2013.05.009
Pesci A, Bonali E, Teza G, Casula G, Boschi E (2012) Metodo basato sulla tecnologia laser scanning per la misura delle deformazioni indotte negli edifici dai sismi o altri eventi distruttivi. In: La Geofisica al servizio della Protezione Civile

Pieraccini M, Dei D, Betti M, Bartoli G, Tucci G, Guardini N (2014) Dynamic identification of historic masonry towers through an expeditious and no-contact approach: application to the "Torre del Mangia" in Siena (Italy). J Cult Herit 15:275–282. doi:10.1016/j.culher.2013.07.006

Ramos LF, Marques L, Lourenço PB, De Roeck G, Campos-Costa A, Roque J (2010) Monitoring historical masonry structures with operational modal analysis: two case studies. Mech Syst Signal Process 24:1291–1305. doi:10.1016/j.ymssp.2010.01.011

Russo S (2013) On the monitoring of historic Anime Sante church damaged by earthquake in L' Aquila. Struct Control Heal Monit. doi:10.1002/stc

Russo G, Bergamo O, Damiani L, Lugato D (2010) Experimental analysis of the "Saint Andrea" Masonry Bell Tower in Venice. A new method for the determination of "Tower Global Young's Modulus E". Eng Struct 32:353–360. doi:10.1016/j.engstruct.2009.08.002

Sabia D, Aoki T, Cosentini RM, Lancellotta R (2015) Model updating to forecast the dynamic behavior of the Ghirlandina Tower in Modena, Italy. J Earthq Eng 19:1–24. doi:10.1080/13632469.2014.962668

Saisi A, Gentile C (2015) Post-earthquake diagnostic investigation of a historic masonry tower. J Cult Herit 16:602–609. doi:10.1016/j.culher.2014.09.002

Van Overschee P, De Moor B (1996) Subspace Identification for linear systems: theory and implementation—applications. Kluwer, Dordrecht



https://dspace.org/

Dynamic investigation on the Mirandola bell tower in post-earthquake scenarios

Zanotti Fragonara, Luca; Boscato, Giosue; Ceravolo, Rosario; Lentile, Silvia; Russo, Salvatore ...

2016-07-19
Springer
https://dspace.lib.cranfield.ac.uk/handle/1826/10678
Zanotti Fragonara L, Boscato G, Ceravolo R, et al., (2017) Dynamic investigation on the Mirandola bell tower in post-earthquake scenarios, Bulletin of Earthquake Engineering, Volume 15, Issue 1, January 2017, pp. 313-337

Downloaded from a DSpace repository. https://dspace.org/